Role of magnetic anisotropy on the magnetic properties of Ni nanoclusters embedded in a ZnO matrix

W. C. Nunes,[1,a)] R. P. Borges,[1,2,b)] M. M. Cruz,[2,3] R. C. da Silva,[4,5] U. Wahl,[5,6] A. Cuchillo,[7] P. Vargas,[8] C. Magen,[9] and M. Godinho[2,3]
[1]*Instituto de Física da Universidade Federal Fluminense, Niterói, 24210-346 Rio de Janeiro, Brazil*
[2]*Centro de Física da Matéria Condensada da Universidade de Lisboa, Campo Grande, 1749-016 Lisboa, Portugal*
[3]*Faculdade de Ciências, Universidade de Lisboa, Campo Grande, 1749-016 Lisboa, Portugal*
[4]*IST/IPFN, Instituto Superior Técnico, Universidade de Lisboa, Campus Tecnológico e Nuclear, E.N.10, 2685-066 Bobadela LRS, Portugal*
[5]*Centro de Física Nuclear da Universidade de Lisboa, Av. Prof. Gama Pinto 2, 1649-003 Lisboa, Portugal*
[6]*IST/C2TN, Instituto Superior Técnico, Universidade de Lisboa, Campus Tecnológico e Nuclear, E.N. 10, 2685-066 Bobadela LRS, Portugal*
[7]*Departamento de Física, Universidad de Atacama, Copiapó, Chile*
[8]*Departamento de Física, Universidad Técnica Federico Santa María Valparaíso, Chile*
[9]*Laboratorio de Microscopías Avanzadas (LMA), Instituto de Nanociencia de Aragón (INA) - ARAID and Departamento de Física de la Materia Condensada, Universidad de Zaragoza, 50018 Zaragoza, Spain*

(Received 9 April 2014; accepted 6 July 2014; published online 18 July 2014)

We have investigated the magnetic properties of Ni nanoaggregates produced by ion implantation in ZnO single crystals. Several deviations from classical models usually adopted to describe the magnetic properties of nanoparticle systems were found. The strain between host and Ni nanoaggregates induces a magnetic anisotropy with a preferred direction. We show that these anisotropy effects can be misinterpreted as a ferromagnetic or antiferromagnetic coupling among the nanoaggregates similar to that of an oriented, interacting nanocrystal ensemble. © *2014 AIP Publishing LLC*. [http://dx.doi.org/10.1063/1.4890498]

I. INTRODUCTION

Nanostructured materials are the key component of many technological systems due their specific physical properties. In particular, magnetic nanoparticles (NPs) have been used for applications in magnetic recording media, ferrofluids, hybrid sensors and for biomedical applications such as drug delivery or magnetic hyperthermia. This makes the understanding of the properties of magnetic nanoparticles one of the leading problems in the study of magnetic materials.

The formation of magnetic NPs embedded in a semiconducting matrix is also important for applications on optical active devices as well as from the point of view of the fundamental physics of nanostructured materials. Recently, doped ZnO is being explored for spintronic applications displaying relevant spin coherence relaxation times.[1] However, the experimental results on doped ZnO strongly depend on the preparation conditions of ZnO and on the doping process, implying different reported results for the electrical and magnetic properties of similar systems. In particular, the room temperature magnetic behavior of transition metal (TM) doped ZnO can vary from paramagnetic[2] to superparamagnetic[3] and ferromagnetic.[4–6] The superparamagnetic behavior is associated with the formation of stable nanosized clusters of the magnetic TM ions even if the clusters are not detected by standard x-ray diffraction. In this respect, ion implantation has been shown to be an appropriate technique for the synthesis of magnetic nanoparticles with controlled size and composition embedded in a crystalline matrix with optical and mechanical functionalities such as ZnO.[7–10]

The physical and chemical properties of the magnetic NPs can be very different from those of their bulk counter-part.[11] Theoretical and experimental studies have recognized that the magnetic anisotropy can be an important factor affecting the magnetic properties of magnetic nanoparticle systems above T_B.[12–14] Vargas *et al.*[13] predicted that the uniaxial anisotropy effect in a system of non-interacting NP with aligned easy magnetization axes can be misinterpreted as a ferromagnetic or antiferromagnetic coupling among the NP, depending on the angle between the anisotropy axes and the magnetic field.

We focus on the magnetic properties of an assembly of texturized Ni aggregates synthesized by ion implantation of single crystals of ZnO and present results for the magnetic anisotropy effects in such systems. The results are discussed considering the role of the magnetic anisotropy on the magnetic properties of oriented nanocrystals according with the prediction of the theoretical model developed by Vargas *et al.*[13]

II. EXPERIMENTAL

ZnO single crystals with dimensions $10 \times 10 \times 0.5\ mm^3$ and (0001) orientation (*c*-axis perpendicular to the crystal surface) were implanted with Ni at 300 K with an implantation energy of 200 keV and fluences of 0.5×10^{17} and $1.0 \times 10^{17}\ cm^{-2}$. Structural characterization of the samples was carried out by Rutherford backscattering spectroscopy (RBS), RBS in combination with the channeling effect and

[a)]Electronic mail: wnunes@if.uff.br.
[b)]Electronic mail: rpborges@if.uff.br.

x-ray diffraction (XRD) and was presented elsewhere.[15,16] Local morphology and structure determination were studied by scanning transmission electron microscopy (STEM) in an FEI Titan 60–300 microscope. Magnetization measurements were performed using a SQUID magnetometer (Quantum Design MPMS). Zero field cooling (ZFC) magnetization was measured upon warming with an external field applied after cooling the system in zero magnetic field. Field cooling (FC) magnetization was measured upon warming under the same applied field used during the cooling.

III. THEORETICAL BACKGROUND

The study of single-domain magnetic systems is based on the uniform rotation of magnetization according to the classical Stoner-Wohlfarth (SW) model.[17] However, the SW model does not consider inter-domain magnetic interactions and does not take explicitly into account thermal fluctuations. The thermal fluctuation of the magnetization of single-domain systems was introduced by Néel and Brown considering uniform magnetization and uniaxial anisotropy.[18,19] In this context, the thermal equilibrium is mediated by thermal fluctuation following the Arrhenius switching probability,

$$\tau = \tau_0 \exp(KV/k_B T), \tag{1}$$

where the characteristic time constant τ_0 is normally taken in the range 10^{-11}–10^{-9} s, k_B is the Boltzmann constant, K is the uniaxial anisotropy constant, and V is the particle volume. KV represents the energy barrier between two easy directions. Bean and Livingston considered that for an assembly of noninteracting single-domain particles at a given observation time (τ_{obs}) there is a critical temperature, called the blocking temperature (T_B), above which the system behaves as a superparamagnet. On the contrary, below T_B the system is said to be blocked. This superparamagnetic approach is widely used in the study of the magnetic properties of nanostructurated magnetic systems. In more recent models, some additional effects such as the magnetic anisotropy and inter-grain magnetic interactions have been included.[20]

A. Temperature dependence of coercive field

The temperature dependence of both coercive field and remanence obtained from the $M(H)$ curves measured at different temperatures can be used to estimate the magnetic anisotropy value.

The $H_C(T)$ behavior for a real system has been described by a simple model in which both blocking temperature distribution and unblocked particles contribution are considered.[21] According to this model, the coercive field of the blocked particles is obtained by means of

$$H_{CB} = \alpha \frac{2K}{M_S}\left[1 - \left(\frac{T}{\langle T_B\rangle_T}\right)^{\frac{1}{2}}\right], \tag{2}$$

where α is a parameter that takes the value $\alpha = 1$ if the particle easy axes are aligned or $\alpha = 0.48$ if randomly oriented.[17,22] $\langle T_B\rangle_T$ is the average blocking temperature, which takes into account only the volume fraction of blocked particles at temperature T.

As any real system has a distribution of particles volume (and consequently a blocking temperature distribution, $f(T_B)$), the total coercive field can be calculated by averaging the magnetization of superparamagnetic and blocked particles, thus yielding

$$\langle H_C\rangle_T = \frac{M_r(T)}{\chi_S(T) + \dfrac{M_r(T)}{H_{CB}(T)}}, \tag{3}$$

where $M_r(T)$ is the remanence for different temperatures and $\chi_S(T)$ the susceptibility of the particles that are superparamagnetic at a certain temperature T. To obtain $\langle H_C\rangle_T$ through Eq. (3), three terms must be determined from experiments: $M_r(T)$, $\chi_S(T)$, and $H_{CB}(T)$.[21,23,24]

IV. RESULTS AND DISCUSSION

In two previous publications,[15,16] we have shown that despite the heavy damage caused by implantation there is no amorphization of the ZnO matrix. Furthermore, the XRD results showed that the Ni forms textured aggregates with one of the ⟨111⟩ directions of Ni parallel to the ⟨0001⟩ direction of ZnO. Below, we will discuss our results with reference to the Ni particles rather than the substrate and when we refer to ⟨111⟩ of Ni we mean only that direction that is parallel to the c-axis of ZnO (or equivalently, perpendicular to the crystal surface).

From the study of the magnetic properties based on the superparamagnetic models, we have estimated the average diameter (D) for the Ni nanoparticles the value of (2.2 ± 0.2) nm and (2.6 ± 0.2) nm for the samples implanted with fluences of 0.5×10^{17} and $1.0 \times 10^{17}\,\mathrm{cm}^{-2}$, respectively. We have also shown that the magnetization curves display a typical behavior of non-interacting single-domain particles. Particle sizes obtained from magnetization are in good agreement with the results of STEM analysis.[16] In Fig. 1, we show Z contrast STEM images obtained for the sample implanted with $0.5 \times 10^{17}\,\mathrm{cm}^{-2}$. Two magnifications of the cross section of the implanted ZnO crystal are shown where we can observe that the particles are formed separated from each other by distances of the order of 5 nm. For such distance and considering, the average magnetic moment of 296 μ_B obtained in Ref. 16, the dipolar interaction is smaller than 0.5 K. For the case of the sample implanted with $1.0 \times 10^{17}\,\mathrm{cm}^{-2}$ the average magnetic moment is 443 μ_B and for a distance of 5 nm the dipolar interaction would be 1 K. This allows us to confidently disregard dipolar interactions between the particles.

The $M(H)$ curves measured at 2.0 K for a sample with a fluence of $1.0 \times 10^{17}\,\mathrm{cm}^{-2}$ for field applied either parallel and perpendicular to the Ni ⟨111⟩ direction are shown in Fig. 2. According to the Stoner and Wohlfarth model for a single-domain particle with uniaxial anisotropy, it is expected that values of H_C and M_r increase as the angle between the applied field and the easy axis decreases. Some features are noticed when we consider the difference between the magnetization measured for different directions of the external magnetic field such as shown in Fig. 2. Most

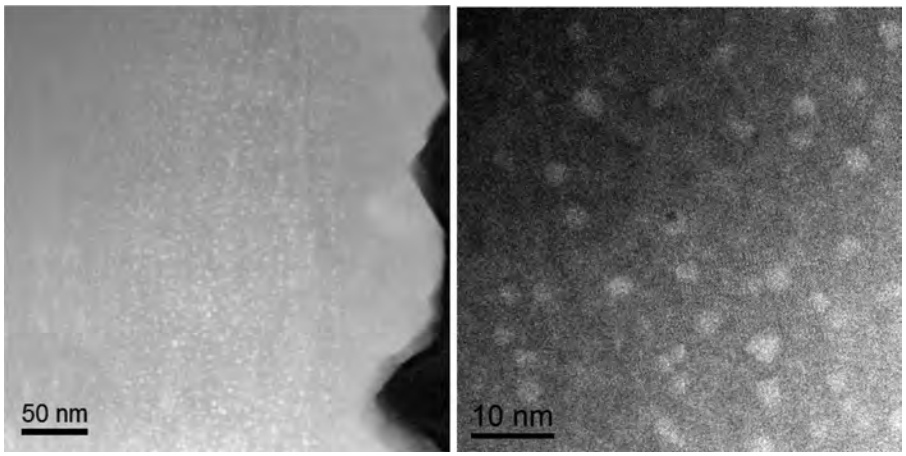

FIG. 1. TEM images showing a cross section of the ZnO crystal implanted with Ni with a fluence of $0.5 \times 10^{17}\,\mathrm{cm}^{-2}$.

noticeably, the $M(H)$ curve taken for external field applied perpendicular to the Ni $\langle 111 \rangle$ direction has the highest M_r and lowest saturation field suggesting that the Ni aggregates have anisotropy with easy magnetization in the plane perpendicular to the Ni $\langle 111 \rangle$ direction. The same features are observed for the sample implanted with $0.5 \times 10^{17}\,\mathrm{cm}^{-2}$.

An individual particle with uniaxial anisotropy has two stable states for the magnetic moment pointing up or down. In real systems even with oriented easy axis (e.g., ensemble of magnetic nanowires) there are other factors such as dipolar interaction, competition of magnetic anisotropy of different origins, that contribute to the total energy resulting in a deviation of the magnetization of the system as a whole from a pure bi-stable magnetic state.[13,25,26] In addition, bulk Ni has a cubic magnetic anisotropy with easy magnetization direction along [111].[27] However, the $M(H)$ results obtained for our samples indicate that the Ni $\langle 111 \rangle$ parallel to $\langle 0001 \rangle$ ZnO axis is a hard direction of magnetization, consequently, one can infer that the magnetic anisotropy of the aggregates is strongly dependent on the interfacing with the host matrix.

In order to obtain more information about the magnetic properties of these systems, the $M(H)$ curves taken at different temperatures were also investigated and are plotted in Fig. 3 for both samples. Figure 4 shows the variation with temperature of M_r for the sample implanted with a fluence of $1.0 \times 10^{17}\,\mathrm{cm}^{-2}$, obtained from the $M(H)$ curves measured at different temperatures. For a system with oriented easy-axes, the remanence is observed to vary according to[28]

$$M_r(T) = \alpha M_r(0)\left[1 - \int_0^T f(T_B)dT_B\right]. \quad (4)$$

Thus, the temperature derivative of the remanent magnetization reflects the distribution of blocking temperature, $f(T_B)$, of the systems. We have considered a log-normal distribution of blocking temperatures to fit Eq. (4) to the temperature dependence of M_r by using the width (σ) and the average blocking temperature $\langle \mathrm{TB} \rangle$ as free parameters. The solid line in Fig. 4 shows the fitting result and the corresponding distribution is shown in the inset of the same figure.

Figures 5(a) and 5(b) show the temperature dependence of H_C of sample $0.5 \times 10^{17}\,\mathrm{cm}^{-2}$ and $1.0 \times 10^{17}\,\mathrm{cm}^{-2}$,

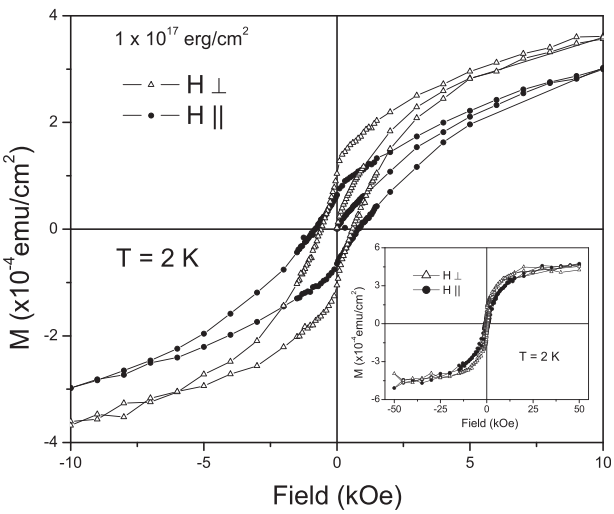

FIG. 2. Magnetization loop curves measured, with the field applied parallel and perpendicular to the Ni $\langle 111 \rangle$ direction, for sample with the fluence of $1.0 \times 10^{17}\,\mathrm{cm}^{-2}$ at 2.0 K. The inset shows the results for the full range of applied magnetic field.

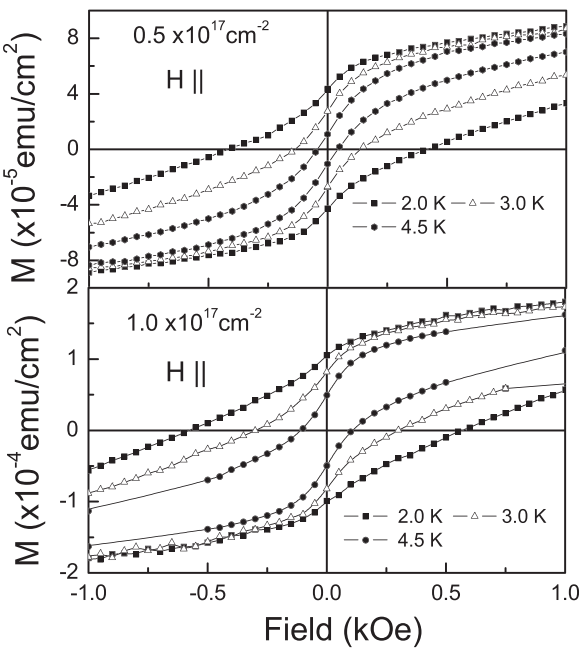

FIG. 3. Magnetization loop curves taken at different temperatures with the field applied parallel to Ni $\langle 111 \rangle$ direction for samples $0.5 \times 10^{17}\,\mathrm{cm}^{-2}$ and $1.0 \times 10^{17}\,\mathrm{cm}^{-2}$.

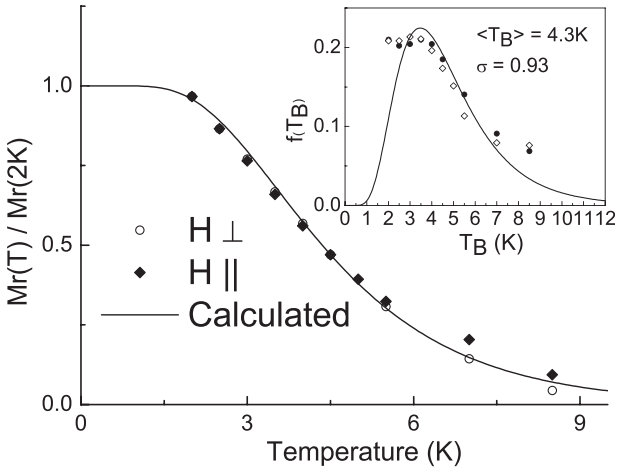

FIG. 4. Remanence vs. temperature obtained for the sample with fluence of $1.0 \times 10^{17}\,\mathrm{cm}^{-2}$. The inset shows distributions of blocking temperatures obtained by derivation of the remanence vs. T curves.

respectively. We can observe that although the temperature dependence of the coercivity is similar for both samples, the values of H_C depend on the direction of magnetization measurement. This result could be related to the texturization of Ni aggregates in the ZnO host according to Eq. (2). Here, we consider that the value of α for the magnetization measured with the magnetic field applied parallel to the Ni $\langle 111 \rangle$ direction ($\alpha_{\|}K$) is different from the one obtained for the magnetization measured with the magnetic field parallel to the surface of the crystal ($\alpha_{\perp}K$). Indeed, we simulated the

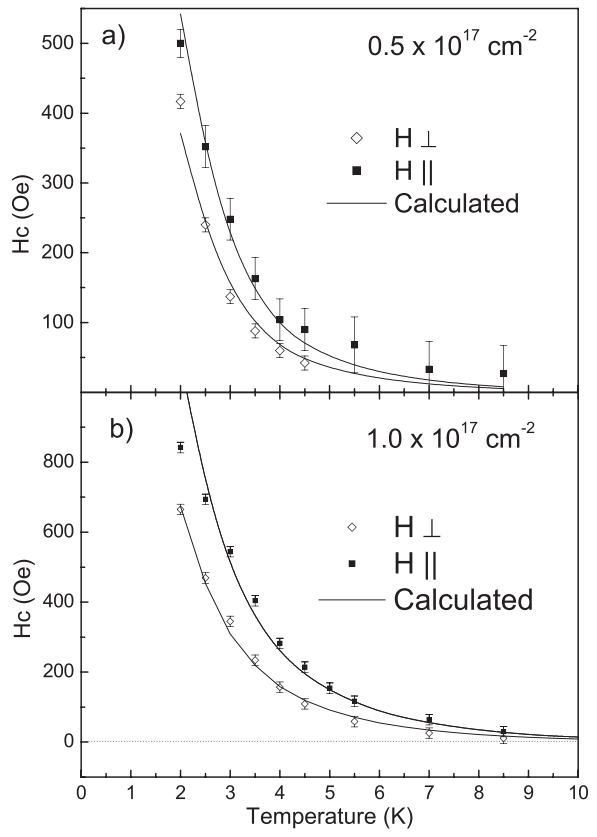

FIG. 5. Coercive field vs. temperature obtained for the samples with fluences of (a) $0.5 \times 10^{17}\,\mathrm{cm}^{-2}$ and (b) $1.0 \times 10^{17}\,\mathrm{cm}^{-2}$.

temperature dependence of $\langle H_C \rangle_T$ using Eqs. (2) and (3), and $f(T_B)$ obtained from M_r curves. The result is plotted as a solid line in Fig. 5. As can be seen, the agreement between theoretical and experimental curves is good for the complete temperature range. A shift between the theoretical and experimental values in such curves has been previously attributed to interparticle interaction effects.[21,24] Here such a shift is not observed, confirming that the intercluster interactions are not an important factor influencing the magnetic properties of our samples. We use $M_S = 485\,\mathrm{emu/cm}^3$ (bulk Ni value),[27] and consequently, the only free parameter used in the fit was the product $\alpha_{\|}K$ ($\alpha_{\perp}K$) for $H_C(T)$ curve obtained from $M(H)$ measured parallel (perpendicular) to the Ni $\langle 111 \rangle$ direction. The numerical values obtained from this analysis are shown in Table I. We found higher values for $\alpha_{\|}$ as compared to $\alpha_{\perp}$ for both samples and the ratio $\alpha_{\perp}/\alpha_{\|}$ is shown in the table. This ratio should vary between 0.48 (all particles have one easy axis parallel to $\langle 111 \rangle$ of Ni and randomly aligned easy axis perpendicular to that direction) and 1 (all easy axes randomly oriented in all directions). In the system studied the ratio $\alpha_{\perp}/\alpha_{\|}$ indicates that the larger particles have hard axis orientations correlated with the $\langle 111 \rangle$ direction parallel to $\langle 0001 \rangle$ of ZnO while for smaller particles this correlation seems to be weaker. Furthermore, the value found for the effective magnetic anisotropy is two orders of magnitude larger than the effective magnetocrystalline anisotropy of bulk Ni (the anisotropy corresponding to the energy barrier between the two easy directions for cubic Ni, that at low temperature is $\frac{K_1}{12} \approx 1.0 \times 10^4\,\mathrm{erg/cm}^3$).[27,29] It is worth mentioning that the fitting parameter in the H_C analysis is M_S/K and by using the Ni bulk value for the saturation magnetization of the particles we are overestimating the value of K although this does not affect the value of the ratio $\alpha_{\perp}/\alpha_{\|}$.

It is well known that the surface anisotropy plays an important role on the magnetic properties of nanoparticles and its relative weight to bulk anisotropy increases as the diameter of the nanoparticles decreases.[30] However, our analysis of coercivity shows that the anisotropy is smaller for the smaller particles, indicating that surface anisotropy is not the dominant term. Magnetoelastic anisotropy has been reported to dominate in systems of transition-metal nanoparticles embedded in ZnO crystal.[8] In fact, mechanical stress can produce remarkable effects on the magnetization behavior of polycrystalline Ni, including a strong change in the magnetic permeability.[27] A strain imposed by the ZnO crystal on Ni aggregates may explain the difference between the magnetization measured for different applied field directions (see Fig. 2). The strain anisotropy energy is given by $E = -\frac{3}{2}\lambda\sigma\cos^2\theta$, where λ is the magnetostriction coefficient ($\lambda_{111} = -24 \times 10^{-6}$ for Ni), σ is the induced strain and θ is the angle between magnetization and the deformation axis.[31] We have estimated the magnetoelastic anisotropy considering the stress imposed by the ZnO matrix on the Ni nanoparticles. The x-ray data show that Ni is strained along the $\langle 111 \rangle$ direction with the distance between (111) planes 1 to 1.5% larger than the bulk value.[15] We find that this tensile strain induces an anisotropy (K_λ) that is much larger than the magnetocrystalline anisotropy of bulk Ni. Since the magnetostriction of Ni is negative, the tensile stress reduces the

TABLE I. Fitting parameters obtained by means of different analysis.

Sample/Fluence	Results obtained by different studies					
	x-ray			Coercive field analysis		
	D (nm)	K_λ (erg/cm^3)[10 K]	K_λ (erg/cm^3)[300 K]	$\alpha_\parallel K$ (erg/cm^3)	$\alpha_\perp K$ (erg/cm^3)	$\alpha_\perp/\alpha_\parallel$
0.5×10^{17} cm^{-2}	2.2 ± 0.2	1.0×10^6	7.1×10^5	4.6×10^5	3.2×10^5	0.70
1.0×10^{17} cm^{-2}	2.6 ± 0.2	6.9×10^5	4.7×10^5	1.2×10^6	5.7×10^5	0.48

permeability in the ⟨111⟩ direction, thus contributing to an easy magnetization in the plane perpendicular to the ⟨111⟩ direction of Ni. If we now consider a direction in the plane of the crystal we expect a compressive strain since the unit cell volume of Ni should remain constant, and therefore a negative σ. A negative σ favours the magnetization lying in the plane of the crystal. We see that analysis of the stress anisotropy energy favours an easy magnetization orientation in the plane of the crystal. The determination of the value of K_λ at room temperature is based on x-ray data while the value at 10 K (see Table I) is an estimate based on the thermal expansion of Ni and ZnO.

To study in more detail, the effect of the anisotropy as a function of temperature, we studied the ZFC and FC magnetization curves taken for different orientations of the external applied field. Figures 6 and 7 show the ZFC and FC curves for samples with fluences of 0.5×10^{17} cm^{-2} and 1.0×10^{17} cm^{-2}, respectively. As can be clearly seen in Fig. 7, ZFC and FC magnetization depends on the orientation of the external applied field, assuming higher values when the field is applied perpendicular to the Ni ⟨111⟩ direction. However, for each sample, the overall shape of the ZFC and FC curves is similar with the same irreversibility temperature and the same blocking temperature independently of the direction of external applied field.

The insets in Figs. 6 and 7 show the inverse susceptibility as a function of temperature for the samples with fluences 0.5×10^{17} cm^{-2} and 1.0×10^{17} cm^{-2}, respectively. For both samples, the extrapolated temperature value resulting from a Curie-Weiss law analysis depends on the orientation between the external applied field and the easy axis. For fields applied perpendicular to ⟨111⟩ of Ni (along the easy axis), the susceptibility curve resembles a system with ferromagnetic-like interactions whereas for fields applied parallel to ⟨111⟩ of Ni (orthogonal to the easy axis), an antiferromagnetic-like coupling is obtained. The reason why this is not so clearly observed for the sample with fluence 0.5×10^{17} cm^{-2} is explained by a deviation of the easy/hard magnetization axis from Ni ⟨111⟩ direction as indicated by the H_C analysis.

A theoretical work by Vargas *et al.*[13] predicted a similar behavior to that observed for our samples, considering the effect of a uniaxial anisotropy on the magnetization of an ensemble of noninteracting single-domain nanoparticles. We have used this model to calculate the susceptibility for a system of noninteracting magnetic single-domain particles considering the effective uniaxial anisotropy value that we obtained from the H_C vs. T analysis. The results are displayed in Fig. 8 for two angles between anisotropy axis and external magnetic field.

The inset of Fig. 8 shows the inverse of the susceptibility as a function of temperature. Although an exact agreement should not be expected when comparing actual experimental data with the predictions of a simplified model as the one shown here, the results agree qualitatively fairly well with our experimental findings, as shown in the insets of the Figs. 6 and 7. Therefore, the shift of the inverse susceptibility towards ferromagnetic-like or antiferromagnetic-like interactions that we observe is surely associated to strain

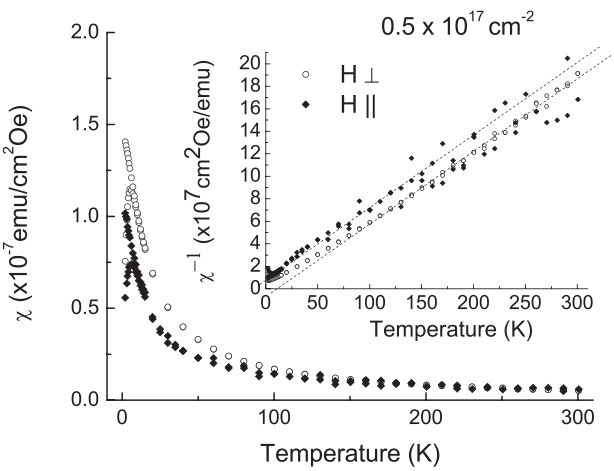

FIG. 6. ZFC and FC curves measured with the field applied both parallel and perpendicular to the Ni⟨111⟩ direction for the sample with fluence of 0.5×10^{17} cm^{-2}. The inset shows the inverse ZFC and FC magnetization curves.

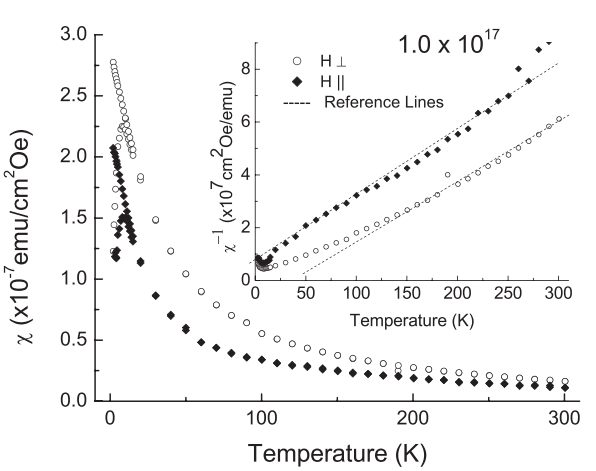

FIG. 7. ZFC and FC curves measured with the field applied both parallel and perpendicular to the Ni ⟨111⟩ direction for the sample with fluence of 1.0×10^{17} cm^{-2}. The inset shows the inverse ZFC and FC magnetization curves.

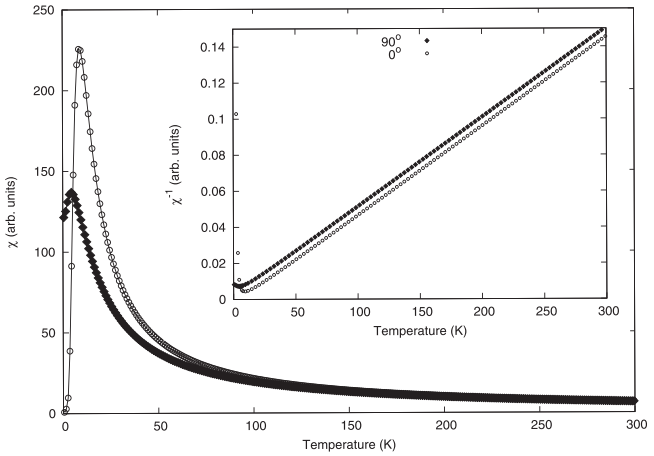

FIG. 8. ZFC curves calculated for a system of non-interacting particles with anisotropy field of 2500 Oe. The two curves represent values of magnetization for different angles between anisotropy axis and applied magnetic field.

anisotropy of Ni nanoaggregates and not to interparticle interactions.

V. CONCLUSIONS

We have investigated the magnetization process of textured Ni nanoparticles embedded in a ZnO single crystal. Both $M(H)$ and ZFC/FC curves exhibit magnetic properties that depend crucially on the direction of measurement. Although the systems have a small nanoparticle size distribution and negligible interaction, we observe that the ZFC/FC magnetization curves above the blocking temperature deviate from the behavior expected for a superparamagnetic system. The results are interpreted considering the role of a strain induced anisotropy that dominates the high temperature magnetization and gives the system a behavior similar to that of an oriented non-interacting uniaxial anisotropy ensemble described by the theoretical model of Vargas and coworkers.

ACKNOWLEDGMENTS

The authors are grateful to FCT for financial support through project PTDC/FIS/66262/2006. W. C. Nunes and R. P. Borges gratefully acknowledge support from Brazilian agencies CNPq, FAPERJ, and CAPES. P. Vargas acknowledges support from Fondecyt Grant No. 1100508. A. Cuchillo acknowledges support from Project DIUDA, ICM Grant No. P10-061-F by FIC-MINECON and Basal Grant No. FB0807.

[1]Z. Yang, Appl. Phys. A **112**, 241 (2013).
[2]Z. Yin, N. Chen, F. Yang, S. Song, C. Chai, J. Zhong, H. Qian, and K. Ibrahim, Solid State Commun. **135**, 430 (2005).
[3]M. Opel, K.-W. Nielsen, S. Bauer, S. T. B. Goennenwein, J. C. Cezar, D. Schmeisser, J. Simon, W. Mader, and R. Gross, Eur. Phys. J. B **63**, 437 (2008).
[4]X. Liu, F. Lin, L. Sun, W. Cheng, X. Ma, and W. Shi, Appl. Phys. Lett. **88**, 062508 (2006).
[5]X. J. Liu, X. Y. Zhu, C. Song, F. Zeng, and F. Pan, J. Phys. D: Appl. Phys. **42**, 035004 (2009).
[6]A. Zukova, A. Teiserskis, S. van Dijken, Y. K. Gun'ko, and V. Kazlauskiene, Appl. Phys. Lett. **89**, 232503 (2006).
[7]R. P. Borges, J. V. Pinto, R. C. da Silva, A. P. Gonçalves, M. M. Cruz, and M. Godinho, J. Magn. Magn. Mater. **316**, e191 (2007).
[8]S. Zhou, K. Potzger, J. von Borany, R. Grotzschel, W. Skorupa, M. Helm, and J. Fassbender, Phys. Rev. B **77**, 035209 (2008).
[9]S. Zhou, K. Potzger, G. Talut, J. von Borany, W. Skorupa, M. Helm, and J. Fassbender, J. Appl. Phys. **103**, 07D530(2008).
[10]M. Schumm, M. Koerdel, S. Müller, C. Ronning, E. Dynowska, Z. Golacki, W. Szuszkiewicz, and J. Geurts, J. Appl. Phys. **105**, 083525 (2009).
[11]J. L. Dormann, D. Fiorani, and E. Tronc, Adv. Chem. Phys. **98**, 283 (1997).
[12]M. Respaud, J. M. Broto, H. Rakoto, A. R. Fert, L. Thomas, B. Bárbara, M. Verelst, E. Snoeck, P. Lecante, A. Mosset, J. Osuna, T. O. Ely, C. Amiens, and B. Chaudret, Phys. Rev. B **57**, 2925 (1998).
[13]P. Vargas, D. Altbir, M. Knobel, and D. Laroze, Europhys. Lett. **58**, 603 (2002); P. Vargas and D. Laroze, J. Magn. Magn. Mater. **272–276**, e1345 (2004).
[14]P. Allia, P. Tiberto, M. Coisson, A. Chiolerio, F. Celegato, F. Vinai, M. Sangermano, L. Suber, and G. Marchegiani, J. Nanopart. Res. **13**, 5615 (2011).
[15]R. P. Borges, B. Ribeiro, A. R. G. Costa, C. Silva, R. C. da Silva, G. Evans, A. P. Gonçalves, M. M. Cruz, M. Godinho, and U. Wahl, Eur. Phys. J. B **79**, 185 (2011); R. P. Borges, B. Ribeiro, A. R. G. Costa, C. Silva, R. C. da Silva, G. Evans, A. P. Gonçalves, M. M. Cruz, M. Godinho, and U. Wahl, *ibid*. **85**, 91 (2012).
[16]R. P. Borges, B. Ribeiro, M. M. Cruz, M. Godinho, U. Wahl, R. C. da Silva, A. P. Gonçalves, and C. Magén, Eur. Phys. J. B **86**, 254 (2013).
[17]E. C. Stoner and E. P. Wohlfarth, Philos. Trans. R. Soc., London, Ser. A **240**, 599 (1948), reprinted by IEEE Trans. Magn. **27**, 3475 (1991).
[18]L. Néel, Ann. Geophys. **5**, 99 (1949).
[19]W. F. Brown, Phys. Rev. **130**, 1677 (1963).
[20]W. C. Nunes, L. M. Socolovsky, J. C. Denardin, F. Cebollada, A. L. Brandl, and M. Knobel, Phys. Rev. B **72**, 212413 (2005).
[21]W. C. Nunes, W. S. D. Folly, J. P. Sinnecker, and M. A. Novak, Phys. Rev. B **70**, 014419 (2004).
[22]C. Bean and J. D. Livingston, J. Appl. Phys. **30**, 120S (1959)
[23]R. W. Chantrell, M. El-Hilo, and K. O'Grady, IEEE Trans. Magn. **27**, 3570 (1991).
[24]W. C. Nunes, F. Cebollada, M. Knobel, and D. Zanchet, J. Appl. Phys. **99**, 08N705 (2006).
[25]D. Laroze, J. Escrig, P. Landeros, D. Altbir, M. Vázquez, and P. Vargas, Nanotechnology **18**, 415708 (2007).
[26]C. Zhu, L. F. Zhang, and C. Xu, J. Magn. Magn. Mater. **320**, 285 (2008).
[27]B. D. Cullity, *Introduction to Magnetic Materials* (Addison-Wesley Publishing Company, Sydney, 1972).
[28]K. O'Grady and R. W. Chantrell, *Magnetic Properties of Fine Particles*, edited by J. L. Dormann and D. Fiorani (North-Holland, Amsterdam), p. 93.
[29]C. de Julián Fernández, Phys. Rev. B **72**, 054438 (2005).
[30]F. Luis, J. M. Torres, L. M. García, J. Bartolomé, J. Stankiewicz, F. Petroff, F. Fettar, J. L. Maurice, and A. Vaurès, Phys. Rev. B **65**, 094409 (2002).
[31]S. Chikazumi, *Physics of Magnetism* (Krieger Publishing Company, Malabar, 1964).